



HAL
open science

Structures of quasicrystals : where are the atoms

Denis Gratias, Marianne Quiquandon

► **To cite this version:**

Denis Gratias, Marianne Quiquandon. Structures of quasicrystals : where are the atoms. *Philosophical Magazine*, 2008, 88 (13-15), pp.1887-1903. <10.1080/14786430801971474>. <hal-00513873>

HAL Id: hal-00513873

<https://hal.science/hal-00513873v1>

Submitted on 1 Sep 2010

HAL is a multi-disciplinary open access archive for the deposit and dissemination of scientific research documents, whether they are published or not. The documents may come from teaching and research institutions in France or abroad, or from public or private research centers.

L'archive ouverte pluridisciplinaire **HAL**, est destinée au dépôt et à la diffusion de documents scientifiques de niveau recherche, publiés ou non, émanant des établissements d'enseignement et de recherche français ou étrangers, des laboratoires publics ou privés.



HAL Authorization



Structures of quasicrystals : where are the atoms

Journal:	<i>Philosophical Magazine & Philosophical Magazine Letters</i>
Manuscript ID:	TPHM-07-Dec-0359.R1
Journal Selection:	Philosophical Magazine
Date Submitted by the Author:	22-Jan-2008
Complete List of Authors:	Gratias, Denis; CNRS-ONERA, LEM Quiquandon, Marianne; CNRS-ONERA, LEM
Keywords:	crystallography, quasicrystals
Keywords (user supplied):	crystallography, quasicrystals
<p>Note: The following files were submitted by the author for peer review, but cannot be converted to PDF. You must view these files (e.g. movies) online.</p>	
DGMQ.tex	



Structures of quasicrystals : where are the atoms

Denis Gratias & Marianne Quiquandon

LEM-CNRS/ONERA, B.P. 72

92322 Châtillon cedex, France

(Received 00 Month 200x; in final form 00 Month 200x)

This paper is an attempt to present a chronological review of the structural concepts that have been developed to characterize quasicrystals, starting from the experimental discovery of D. Shechtman [1] and the concomitant theoretical definition of *quasicrystal* as proposed by D. Levine and P. Steinhardt [2], up to the present research in the field. The largest part of the paper is a discussion of the specific points that make the atomic structure determination of quasicrystals an original and difficult scientific challenge. We finally discuss the soundness of our knowledge of the actual atomic structure in quasicrystals: a quite solid idea of where the atoms are but a not yet secure vision of the chemical species distribution.

1 Introduction

Quasicrystal as introduced by D. Levine and P. Steinhardt [2] in 1984, stands for *quasiperiodic crystal*. Quasiperiodicity, a natural extension of periodicity, is a special case of almost-periodicity (see the basic articles by H. Bohr [3] and A. Besicovic [4]). Beyond this mathematical definition, the experimental recognition of a quasicrystal is in fact a formidable difficult task. We all know what quasicrystals are but we have no satisfactory complete answer of what define them in the most general and fundamental sense (see for instance [5] and the tentative definition by the IUCr [6]).

Our purpose here is to discuss some of the concepts specific to quasicrystals that have emerged during these twenty five years of research. After a short recall of some of the milestones of the history of quasicrystals, we will focus our attention on the N -dim crystallography as the simplest efficient geometrical realization of D. Mermin's approach [7] on the general notion of symmetries. We shall recall some of the geometrical constraints that should be considered in that context for describing real quasicrystals with models that are plausible idealizations of real objects.

The complete atomic structure determination goes through the final crucial step of structure refinement [8] as intensively developed by the group of A. Yamamoto (see, for instance [9]). Final refinement on quasicrystals are today comparable in accuracy with those obtained for standard crystals. Our present point of view is different: simple idealized unrelaxed models are very useful as well — and to some aspects more tractable— for discussing most of the physical properties. We will illustrate that point on two different examples both on the *i*-AlPdMn icosahedral phase. The first one is a discussion of how the specific network of Mn atoms that we recently proposed [10] for the modeling of *i*-AlPdMn can consistently explain both experimental and theoretical works on the magnetic properties of this alloy. Our second example is to discuss how simple idealized models may play an important role in the understanding of the atomic structure of the termination planes in surface studies.

Our global conclusion is that although the actually available models differ on details, they all agree for the locations in space of roughly 85% of the atoms. This comes from the strong experimental evidence of where the major atomic surfaces are located in high dimensional space. The question is still opened for characterizing the location of the remaining atoms and of course for the relaxations from the ideal positions of the overall atoms. The problem is much more delicate concerning the actual distribution of the atomic species on these positions. Various models exist, exhibiting quite similar diffraction patterns, that differ on the chemistry decoration of the atomic sites. There, the debate is still widely opened.

Philosophical Magazine

ISSN 1478-6435 print/ISSN 1478-6443 online © 200x Taylor & Francis

<http://www.tandf.co.uk/journals>

DOI: 10.1080/1478643YYxxxxxxx

1.1 *Historical*

D. Shechtman discovered the icosahedral quasicrystals in early April 1982 with transmission electron microscopy (TEM) observations of a rapidly solidified (Al,Mn) alloy. This observation has first been reported in a long paper by D. Shechtman and I. Blech [11] but published in 1985, whereas the first published in 1984 is the famous paper [1] of the Physical Review Letters. Its theoretical counterpart is to be found in the same journal issue: it is the article of D. Levine and P. Steinhardt [2] who introduced the name *quasicrystal* to designate this new kind of ordered solids. These two papers are considered as the starting point of the research on quasicrystals.

The geometrical link to almost-periodicity and quasiperiodicity (see [3,4]) came very quickly with the introduction, a few months later, of the cut and project method [12–14] and the demonstration [15,16] of the equivalence of these techniques with the former hyperspace cut construction [17] initially invented by P. M. de Wolff [18] for describing incommensurate structures.

Once these bases have been posed in early 1985, two main directions emerged in the problem of deciphering the atomic structures of quasicrystals. A first natural approach was to take the extreme sharpness of the diffraction peaks as the main basic property of these materials (as opposed to glasses) and assume that the atomic structures should be described in the spirit of crystallography with the notion of ideal quasicrystal exemplified by the models generated by the cut method. This generated the so called N -dim crystallography approach [19]. The second approach was based on the idea that quasicrystals should be stabilized mainly through the entropy term of the free energy; this was the random tiling model. It turned out that the famous article of L. Pauling [20] — in which he denied the possible existence of icosahedral quasicrystals — had several side effects, one being of significantly restraining the development of crystallographic research during the 90's. An indirect consequence of that has been the emergence of theories based on the fascinating idea of random tiling especially in the United States. It is interesting to notice that the very first atomistic model proposed by D. Shechtman and I. Blech [11] was indeed based on the remark that the vertices of randomly distributed identical icosahedra in the same orientation and linked by edges, have coordinates x_p that can all be written as *integer* linear combination of the six basic vectors e_i from the center to the vertices and defining the 5-fold directions of the icosahedron: $x_p = \sum_i^N n_i e_i$, $n_i \in \mathbb{Z}$. The complementary study of P. W. Stephens and A. I. Goldman [21] showed the first computed simulation of diffraction pattern of these *icosahedral glasses* with astonishingly well-defined sharp peaks. Random tiling theories took real physical maturation in the early 90's (see for instance [22–26]) and are at the basis of the development of the mathematical studies of covering properties of tilings (see for instance [27–31]). Ideal quasicrystals and random tilings have sometimes been presented as antagonist models. They are in fact the two natural sides of the free energy and have to be considered together.

2 Requisite for a deterministic structure

There are today plentiful stable or metastable quasicrystalline phases in alloys as exhaustively listed until 2004 in the remarkable and complete review by W. Steurer [32]. Whatever point of view is chosen, a reference ideal structure must be introduced at some stage to describe quasicrystals in the context of deterministic long range ordered structures. This is a requisite for giving a sense to P. Bak's famous question "where are the atoms" [33].

2.1 *Essentially discrete diffraction pattern*

The property that was at the basis of D. Shechtman's discovery, is the fact that the diffraction patterns show an *essentially discrete set* of peaks¹ exhibiting forbidden symmetry. This is necessary to allow for individualizing each diffraction spot in *indexing* it with a finite number of integers in an *unambiguous* fashion. Indexation of quasicrystals [34, 35] has been a very crucial step in the understanding of these

¹A dense set of peaks such that peaks with an intensity greater than any strictly positive threshold is discrete.

structures: the logical way to rationally characterize the wave vectors \vec{Q} in reciprocal space as *integer* linear combinations of a finite number N of constant basic unit q_i -vectors, $\vec{Q} = \sum_i^N n_i \vec{q}_i$, $n_i \in \mathbb{Z}$. This defines a so-called \mathbb{Z} -module². The experimentally accessible rank N of this diffraction \mathbb{Z} -module is the number of arithmetically independent unit vectors with which each reflection has an *unique* indexation.

2.2 Non crystallographic symmetries

Non crystallographic symmetries are at the starting point of one of the most important concept developed with quasicrystals : a profound revision of the notion of symmetry proposed by D. Mermin [7], following an original work of A. Bienenstock and P. P. Ewald [36] on the representation of space groups in reciprocal space. It consists in revisiting the notion of geometrical equivalence using the point of view of the physicist. Usual space symmetry operations are geometrical isometries that superimpose objects on top of themselves.

D. Mermin's point of view is to define symmetries through *indistinguishability* rather than simple *superimposition*: any two structures defined by density functions $\rho(r)$ and $\rho'(r)$ are indistinguishable if their correlation functions to any finite order N , $c(r_1, r_2, \dots, r_N)$ and $c'(r_1, r_2, \dots, r_N)$ are identical, *i.e.* if:

$$\int \rho(r_1 - r) \dots \rho(r_N - r) d^3 r = \int \rho'(r_1 - r) \dots \rho'(r_N - r) d^3 r$$

that translates in reciprocal space into the basic relation $\prod_{i=1}^P \hat{\rho}(k_i) = \prod_{i=1}^P \hat{\rho}'(k_i)$ for all closed path of P -th order, $\sum_i^P k_i = 0$, where the k_i -vectors belong to the Fourier carrier of the density function. This relation introduces a linear phase gauge in the Fourier coefficients and leads to a powerful general method of construction of space-groups in Euclidean spaces of any finite dimension [7].

The framework of N -dim crystallography appears as a natural and simple way of realizing the linear phase gauge invariance imposed by the indistinguishability property.

3 N -dim crystallography

Consistently with the definition of quasiperiodicity, N -dim crystallography allows to describe quasicrystals in a Euclidean space of dimension $N > 3$ large enough for recovering periodicity and containing the usual euclidean vector space representation in \mathbf{E}_{\parallel} , but small enough for the hyper-lattice to project in a *uniformly dense* fashion on the internal space \mathbf{E}_{\perp} . In that context, the gauge phase invariance is given by the scalar products $q_{\perp} \cdot t_{\perp}$ where q_{\perp} is the perpendicular component of the N -dim wave vector Q belonging to the N -dim reciprocal lattice Λ^* and t_{\perp} any translation in \mathbf{E}_{\perp} .

This gauge invariance is correlated with the fact that translating the cut by t_{\perp} parallel to itself generates D -dim quasiperiodic structures that are locally isomorphic¹ and have same Fourier coefficients up to the phase factors $\chi(Q) = q_{\perp} \cdot t_{\perp}$.

A crystalline structure is defined by a space group, an unit cell (parameters and angles), and a finite collection of Wyckoff positions corresponding to the various orbits of the atomic species of the crystal. The same holds for quasicrystals except concerning the definition of the *Wyckoff positions*. These are atomic surfaces (AS), also called acceptance windows, that are $(N - D)$ -dim manifolds. They require *a priori* an infinite number of continuous parameters to be characterized, thus ruining the hope of describing *ab initio* a quasicrystal structure with a finite number of data. Additional constraints have to be introduced to reduce the number of parameters to a finite set. These additional requirements should be issued from plausible and acceptable physical conditions that can help for predicting the physical properties and for understanding the nucleation and growth mechanisms of quasicrystals.

²A \mathbb{Z} -module is a vector space built on a ring; it can equivalently be seen as the projection in a space of dimension d along an irrational direction of a regular periodic lattice embedded in a space of dimension $N > d$; N is the rank of the \mathbb{Z} -module.

¹When the N -dim lattice projects uniformly densely in \mathbf{E}_{\perp} , any finite patch of tiles which appears in a given tiling appears in any other tiling defined by a cut parallel to the initial one and with the same frequency.

3.1 Geometrical constraints on the AS

The works on geometrical constraints on ASs are numerous. Detailed demonstrations can be found for example in references [37,38]. The first constraint that can be introduced is *structural simplicity*: like in usual crystals the structure should show finite local complexity in the sense that each atom has a finite number of different local environments to any finite size². The property of finite local complexity makes possible the description of the atomic structure by the knowledge of the *atlas* of the atomic configurations of finite size together with their occurrence frequencies. The more atoms are taken into account in these configurations, the finer the description is.

This requirement of finite local complexity implies the atomic surfaces being $N - D$ volumes *piecewise parallel* to \mathbf{E}_\perp . Thus, quasiperiodic atomic structures share many properties with quasiperiodic *tilings* that appear as underlying skeletons of the atomic structures (like lattices in regular crystals).

The second requirement is based on the idea that quasicrystals are considered as belonging to the possible structural solutions that solids can take for minimizing their internal energy. Indeed, archetypal tilings are known that have local matching rules¹ and can therefore be viewed as possible ground states for some hypothetical finite range interaction Hamiltonians.

Works on matching rules in tiling theory have been very intensive in the 90's (see for instance A. Katz [39] and references herein). Their existence is closely related to the way the cut space intersects rational (hyper)-planes family sustained by the N -dim lattice that should never be crossed by \mathbf{E}_\parallel . These forbidden planes must be numerous enough for forcing the cut space to be oriented in an unique way. Forbidden planes for the icosahedral case are mirror planes of $m\bar{3}5$ and matching rules can be found in tilings generated by ASs bounded by mirror planes *i.e.* polyhedra (a good way to increase the compacity of the model).

The third and last constraint comes from the fact that it has been early recognized that matching rules are not growth rules since the growth process is fundamentally non local. The real structures grow from melt of the alloys and present a strong quasicrystalline perfection. We therefore assume that the atomic jumps necessary to locally recover the ideal quasiperiodic stacking should be of low energy. This means that these jumps occur on small or very small distances. This is the aim of the closeness condition² that is satisfied for polyhedral ASs with vertices located in \mathbf{E}_\perp on points that are rationally scaled with respect to the \mathbb{Z} -module of the projected hyper-lattice.

All together, these constraints suggest constructing AS for the icosahedral phase as polyhedra resulting from intersections, unions and/or rescaling by any number of the form $(n + m\tau)/d, n, m \in \mathbb{Z}, d \in \mathbb{N}^+$ of the eight polyhedra defined by the elementary tessellation under the point group $m\bar{3}5$ (or any subgroup of $m\bar{3}5$) of the mirror planes perpendicular to the 2-fold axes.

3.2 Diffraction

Diffraction is the fundamental tool for quasicrystal structure determination. A general discussion [40] has been proposed several years ago on the diffraction obtained by the cut-and-project methods. The generalization consists in having a cut space \mathbf{E}_c different from the parallel space \mathbf{E}_\parallel and the space \mathbf{E}_σ of the ASs different from \mathbf{E}_\perp . There, a prototypic atomic surface σ is copied at each lattice node (the method extends trivially to several atomic surfaces per unit cell), intersection of this ensemble is taken with a subspace \mathbf{E}_c , and finally the collected points are projected onto \mathbf{E}_\parallel along \mathbf{E}_\perp . A rational orientation of \mathbf{E}_c with respect to Λ generates a periodic structure (1-, 2- or 3-D) made of a periodic collection of atomic clusters where atoms are in general at locations which are *incommensurate* with the lattice parameters. A rational orientation of \mathbf{E}_σ leads to a *quasiperiodic* selection of atomic sites distributing on the nodes of a host *periodic* lattice. In that scheme, the main geometric features of the diffraction spectra are the

²This requirement is not fulfilled in incommensurate structures and could be one of the *distingo* between quasicrystals and incommensurate phases.

¹We say that a tiling has matching rules if there exists a set of local constraints that enforce quasiperiodicity of the tiling as soon as they are satisfied everywhere in the tiling.

²For allowing an easy bulk reconstruction, the cut should easily "glide" in the 6D space along \mathbf{E}_\perp in exploring the class of the indistinguishable structures through low energy atomic jumps with no transport of matter at long distances.

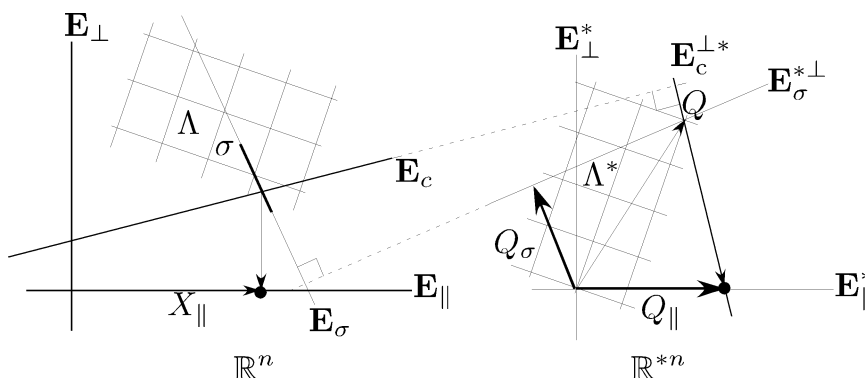


Figure 1. on the left: An interesting version of the cut method consists in intersecting the ASs σ by a cut space \mathbf{E}_c and projecting the intersection points into \mathbf{E}_\parallel along \mathbf{E}_\perp . on the right: the reciprocal space geometry shows that the diffraction peaks are located at the points of projection of Λ^* into \mathbf{E}_\parallel^* along $\mathbf{E}_c^{\perp*}$. The amplitudes of the reflections are given by the characteristic function of the AS σ with the argument given by the projections of Λ^* nodes along $\mathbf{E}_\sigma^{\perp*}$ into \mathbf{E}_σ^* .

following:

- (i) the locations of the peaks in the diffraction pattern depend on the orientation of the lattice Λ with respect to both \mathbf{E}_c and \mathbf{E}_\parallel *irrespectively*¹ of the direction of \mathbf{E}_σ .
- (ii) the intensities of the peaks depend primarily on \mathbf{E}_σ and on \mathbf{E}_c as a secondary effect except if \mathbf{E}_c is rationally oriented.

This shows how quasicrystal structure refinements are carried out. As in standard crystallography, we assume that the locations of the diffraction peaks are given. This leads to fix the lattice Λ , the spaces \mathbf{E}_\parallel , \mathbf{E}_\perp and \mathbf{E}_c . Symmetry requirements usually lead to unique solutions for these items with no possible adjustable parameters. Thus, the remaining possible fit variables are the number, positions and shapes (within the symmetry class) of the AS's and their chemical occupancy factors, in a way similar to usual crystallography.

4 Determination of real structures

Diffraction experiments on good quality single quasicrystals have been carried out starting early 90's for both x-rays and neutrons. The observed intensities correspond to the square of the structure factors $f(Q)$ given by:

$$f(Q) = \sum_j^P f_j(Q_\parallel) \hat{\eta}(Q_\perp) e^{2i\pi Q \cdot R_j}$$

where P is the number of AS's defining the structure in the elementary unit cell, $f_j(Q_\parallel)$ the atomic form factor of the chemical species associated to the j -th AS, $\hat{\eta}(Q_\perp)$ the Fourier transform of the characteristic functions of the ASs and R_j the location of the AS in the unit cell.

For specific R_j with simple rational coordinates the phase factors $e^{2i\pi Q \cdot R_j}$ take simple values and the global structure factors can be written as additions and/or subtractions of the scatterers issued from the various AS as shown on table 1. Indeed, an AS located at R is reproduced by symmetry at all other equivalent sites on the unit cell, the number of which is given by the order of the little group of R , say G_R into the point group, say G , of the quasicrystal: $\nu = |G|/|G_R|$. The set of equivalent vectors are defined by the coset decomposition of G onto G_R , $\mathcal{G} = \bigcup_{i=1}^\nu g_i G_R$, and given by the collection of the ν vectors $g_j R$.

¹Even if \mathbf{E}_σ is rationally oriented, that generates a quasiperiodic decoration of an usual (periodic) lattice, the carrier of the Fourier transform is a non-crystallographic \mathbb{Z} -module. This fact that the Fourier spectrum can have a carrier that is *not* based on the reciprocal lattice of the host lattice is because the quasiperiodic decoration is not the convolution of a finite pattern with the host lattice.

R	little group G_R	coset order ν	$Y(Q)$
$n = (0, 0, 0, 0, 0, 0)$ (F,P)	$m35$	1	1
$n' = (1, 0, 0, 0, 0, 0)$ (F)	$m35$	1	$(-1)^N$
$bc = (\bar{1}, 1, 1, 1, 1, \bar{1})/2$ (F, P)	$m35$	1	$(-1)^M$
$bc' = (1, 1, 1, 1, 1, \bar{1})/2$ (F, P)	$m35$	1	$(-1)^{N+M}$
$me = (1/2, 0, 0, 0, 0, 0)$ (F)	$5m$	12	$1/6 \sum_{j=1}^6 \cos \pi n_j$
$me = (1/2, 0, 0, 0, 0, 0)$ (P)	$\bar{5}m$	6	$1/6 \sum_{j=1}^6 (-1)^{n_j}$

Table 1. Global phase change $Y(Q)$ for a reflection $Q = [N, M](n_1, n_2, n_3, n_4, n_5, n_6)$ due to the location an AS at point R for the F(2A) and P(A)-type icosahedral phases calculated using formula 1. The integers N and M are characteristics of the reflection Q (see J. W. Cahn *et al.* [35]).

The global phase factor $Y(Q)$ attributed to one AS located at R is therefore:

$$Y(Q) = \frac{|G_R|}{|G|} \sum_{i=1}^{\nu} e^{2i\pi Q \cdot g_i R} \tag{1}$$

The first analysis of M. Cornier-Quiquandon *et al.* [41] in AlCuFe has shown that the intensities of the reflections collected for *i*-AlCuFe (that applies as well for *i*-AlPdMn as shown by M. Boudard *et al.* [42]) distribute in four branches when plotted as a function of $|Q_{\perp}|$. Each branch is characteristic of the parities of the two integers N and M defined by J. W. Cahn *et al.* [35] for indexing the diffraction patterns of the icosahedral phases¹. This splitting into four families is the signature of the structure of *i*-AlCuFe (and *i*-AlPdMn) being primarily made of three AS's located at the special points $n = (0, 0, 0, 0, 0, 0)$, $n' = (1, 0, 0, 0, 0, 0)$ and $bc = 1/2(\bar{1}, 1, 1, 1, 1, \bar{1})$, the site bc' being empty for steric reasons.

Moreover, using the fact that the characteristic functions $\hat{\eta}(Q_{\perp})$ are positive values for small $|Q_{\perp}|$ (converging to the value of the volume of the corresponding AS for $|Q_{\perp}| \rightarrow 0$), a simple examination of the experimental intensities leads to assert that there are two large ASs at n and n' (the largest on n) and one small² at bc with $n = (0, 0, 0, 0, 0, 0)$, $n' = (1, 0, 0, 0, 0, 0)$ and $bc = (\bar{1}, 1, 1, 1, 1, \bar{1})/2$ in the notations of J. W. Cahn *et al.* [35].

Some structures with A parameters larger than 0.67 nm like *i*-AlLiCu, *i*-CdYb and *i*-ZnMgHo have additional small atomic surfaces located at the mid-edge $me = (1/2, 0, 0, 0, 0, 0)$. They do not contribute to the amplitudes of reflections Q with N odd — the sub-lattice generated by these ASs is a primitive lattice — and contribute to all others with even N , for both F and P type structures, proportionally to the difference between the number of even n_i minus the number of odd n_i of the reflection Q as:

$$Y(Q) = 1 - 1/3 \sum_j (n_j \pmod{2})$$

that runs between -1 for reflections with all odd indices to +1 for reflections with all even indices by step of 1/3.

All structural determinations of icosahedral quasicrystals so far share this basic property of having high symmetry ASs on the $m35$ special points (plus the mid-edges for some of them). These are strong results because they are based on *purely geometrical arguments* in the interpretation of the diffraction data and that do not rely on modelling hypotheses. This is the main reason why all these structural models share roughly 85% of the atom locations. Of course, tiny differences appear between models according to the exact shape of these three main AS's but they are not very critical for the basic understanding of the atomic structure.

¹Expressing the coordinates of a reflection Q in the internal basis of \mathbf{E}_{\parallel}^* as $Q = \kappa(h + h'\tau, k + k'\tau, \ell + \ell'\tau)$, with $\kappa = 1/\sqrt{2(2 + \tau)}$, $h, h', k, k', \ell, \ell' \in \mathbb{Z}$, leads to define the two numbers $N = h^2 + h'^2 + k^2 + k'^2 + \ell^2 + \ell'^2$ and $M = h'^2 + k'^2 + \ell'^2 + 2(hh' + kk' + \ell\ell')$ that define the length of the reflection Q in \mathbf{E}_{\parallel}^* and \mathbf{E}_{\perp}^* : $|Q_{\parallel}|^2 = \kappa^2(N + M\tau)$ and $|Q_{\perp}|^2 = \kappa^2\tau(N\tau - M)$.

²For avoiding confusion between the two bc positions, the occupied one has the same parity as the smallest of the two AS's of the nodes.

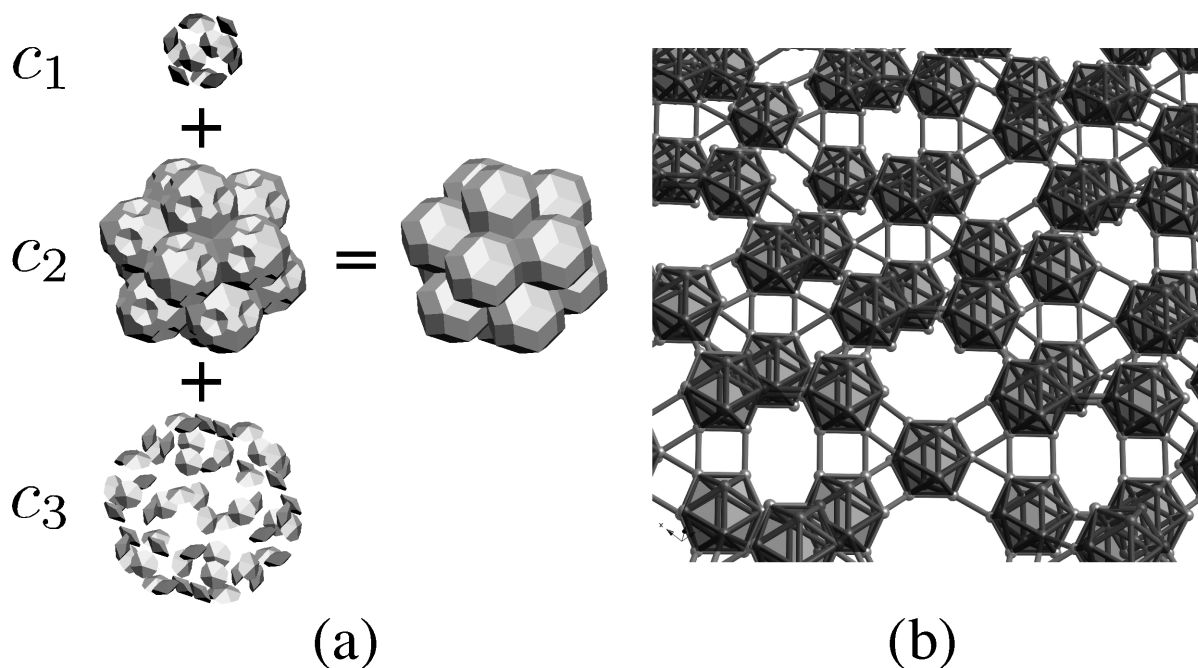


Figure 2. (a) The cell α is made of three elementary cells of the $M(M')$ decomposition. The initial model [10] assigns Mn atoms to the cells $c_2 + c_3$ on the n AS. Here, as a geometrical simplification, we take all 3 subcells together to generate the Mn atoms in i -AlPdMn; the Mn global composition passes thus from 8.29 to 8.42 at %. (b) Corresponding network: a set of identical parallel icosahedra (the large icosahedra of the M clusters) linked by squares with edge length 0.48 nm.

4.1 Chemical ordering

The question that remains opened and that cannot be answered with the same ease, is the determination of the chemical order of these atomic sites. Determining the chemical distribution within the previous ASs is indeed a matter of refinement: no pure geometrical argument can make the decision: several distributions of a given fixed composition coupled with atomic position relaxations are tested against the experimental values in an iterative process that is driven by the comparison with the diffraction data. A difficult point is that, because of the very numerous possible fit parameters (up to several hundreds, see for example [9]), the uniqueness of the solution cannot be guaranteed and other different solutions can definitely not be ruled out.

We shall illustrate here a different approach that is closest to generic geometrical arguments. It consists in constructing an *ab initio* chemical decoration, made as simple as possible, with no fit parameters, based on the hypothesis of *the same chemical species occupy the same kind of local environments*. The alloy composition is then governed by the relative frequencies of these local configurations. Such a model has been recently proposed by the present authors [10] to define at once the various icosahedral structures of type F with the three main atomic surfaces. The details of the model being given elsewhere [10], our only point of interest here is the way the Mn atoms distribute in space in the case of i -AlPdMn.

Here, the Mn atoms are generated by the cell α (shown on figure 2) of the n AS. Its total volume is $-36 + 24\tau$ corresponding to $(-36 + 24\tau)/(11 + 14\tau) = 8.43$ at% of the model. It is made of three elementary subcells shown on figure 2 : c_1 of volume $68 - 42\tau$ corresponds to those Mn atoms (0.12 at %) of the M' icosahedra that are also centers of M clusters, c_3 of volume $340 - 210\tau$ (0.632 at%) corresponding to Mn atoms that also belong to M icosidodecahedra and finally c_2 of volume $-444 + 276\tau$ (7.66 at%) corresponding to Mn atoms that are solely on M' icosahedra. In the original model [10], the Mn cell is made of $c_2 + c_3$ to possibly introduce vacancies on the M' -centers. This lead to a Mn composition of 8.29 at. %. Here, we consider the complete cell α by adding c_1 , 0.12 % in the Mn composition, a too small value for being experimentally measured. Hence, Mn atoms are located on *all* vertices of the large icosahedra of the M' clusters. The icosahedra are connected by bounds that form squares as show on figure 2.

cell	Volume	Frequency (%)	chemical composition
C_1	$-40 + 26\tau$	74.15	5 Al
C_2	$10 - 6\tau$	10.46	5 Al + 1 Pd
C_3	$-74 + 46\tau$	15.40	5 Al + 2 Pd

Table 2. Chemical configurations of neighbors atoms around the Mn atoms of the Mn network. The average coordination between two nearest neighbors Mn atoms at 0.48 nm is $\bar{Z} = (15 + 2\tau)/3 = 6.078$. The second neighbors Mn-Mn interatomic distance is 0.678 nm with an average coordination number of $\bar{Z} = 2\tau/3 = 1.079$.

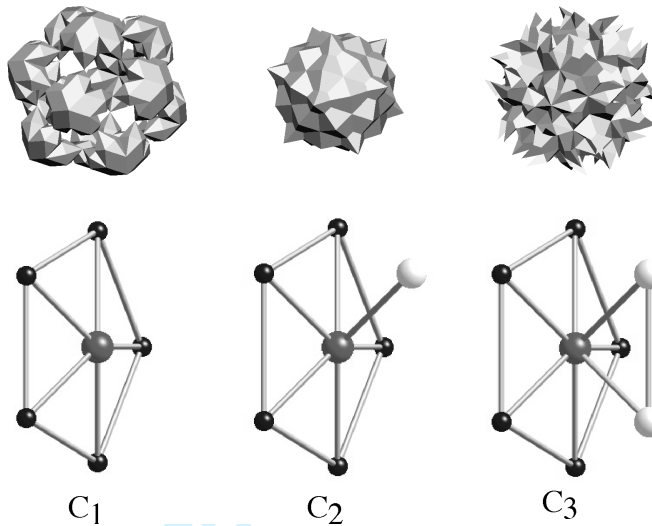


Figure 3. The 3 Mn configurations for first neighbors Mn-Mn interatomic distance (0.48 nm) on the network α . There are 18 configurations in including the second neighbors distance (0.678 nm).

The average number of Mn-Mn first neighbors at 0.48 nm from a central Mn atom is $Z_{Mn} = (15 + 2\tau)/3 = 6.078$. The Mn atoms are distributed on three classes as shown on figure 3 and table 2:

- 34.84% $((-6 + 5\tau)/6)$ have 5 Mn neighbors and are not connected to other icosahedra;
- 22.5% $((12 - 7\tau)/3)$ have 6 Mn neighbors and are connected to one other icosahedron;
- 42.7% $((-4 + 3\tau)/2)$ have 7 Mn neighbors and are connected to two other icosahedra.

The second neighbors distance on the network is 0.678 nm with a coordination of $\bar{Z} = 2\tau/3 = 1.079$.

The analysis of the complete chemical local environment in *i*-AlPdMn shows in table 3 that the Mn atoms have a first coordination shell of $\bar{Z} = (267 - 74\tau)/12 = 12.372$ atoms that distributes between 11.241 Al and 1.1366 Pd, on the three distances 0.2567, 0.2819 and 0.2964 nm according to :

- at the shortest distance 0.2567 nm, $\bar{Z} = (31 + \tau)/6 = 5.4363$ with $\bar{Z}_{Al} = (7 + 5\tau)/3 = 5.03$ et $\bar{Z}_{Pd} = (17 - 9\tau)/6 = 0.4063$;
- at 0.2819 nm, only Pd atoms are found issued from a *bc* AS with an average coordination $\bar{Z}_{Pd} = (6 - \tau)/6 = 0.73033$;
- finally at 0.2964 nm, generated by an AS at *n*, one finds pure aluminum with an average coordination $\bar{Z}_{Al} = (81 - 4\tau)/12 = 6.2106$.

The second neighbors shell is at 0.4561 nm. It is made of atoms located on the large icosahedron of edge length 0.48 nm. It has four configurations with an average coordination $\bar{Z} = (66 + \tau)/6 = 11.27$ that distributes on $\bar{Z}_{Al} = (15 + 2\tau)/3 = 6.07$ for Al and $\bar{Z}_{Pd} = (12 - \tau)/2 = 5.2$ for Pd.

It is very interesting to compare this model with theoretical [43] and experimental [44–47] work on the magnetism in *i*-AlPdMn.

The first remarkable point is that the cell α generates a network of sites with one unique first neighbors distance of 0.48 nm for a maximum atomic composition of 8.4%. This is to be compared to the fact that no magnetic Mn-Mn interactions are observed for Mn content smaller than 8.4%.

The second point is that, in the model, Mn atoms are essentially surrounded by Al atoms (see figure

cell	Volume	Frequency (%)	Z	at 0.2566 nm	0.282 nm	0.2964 nm
C_1	$-66 + 42\tau$	69.10	13	5 Al	1 Pd	7 Al
C_2	$52 - 32\tau$	7.87	12	5 Al + 1 Pd	-	6 Al
C_3	$-16 + 10\tau$	6.37	12	5 Al + 2 Pd	-	5 Al
C_4	$-42 + 26\tau$	2.43	11	5 Al + 2 Pd	-	4 Al
C_5	$13 - 8\tau$	1.97	11	5 Al	1 Pd	5 Al
C_6	$13 - 8\tau$	1.97	12	5 Al	1 Pd	6 Al
C_7	$13 - 8\tau$	1.97	10	5 Al + 2 Pd	-	3 Al
C_8	$13 - 8\tau$	1.97	9	5 Al + 2 Pd	-	2 Al
C_9	$13 - 8\tau$	1.97	11	5 Al + 1 Pd	-	5 Al
C_{10}	$68 - 42\tau$	1.50	7	7 Al	-	-
C_{12}	$68 - 42\tau$	1.50	10	5 Al + 2 Pd	-	3 Al
C_{13}	$-110 + 68\tau$	0.93	8	5 Al + 2 Pd	-	1 Al
C_{14}	$-55 + 34\tau$	0.46	10	5 Al + 1 Pd	-	4 Al

Table 3. Chemical configurations of first neighbors around the Mn atoms of the full i -AlPdMn structural model. The average coordination on the shell is $\bar{Z} = 12.372$ with 11.241 Al and 1.1366 Pd.

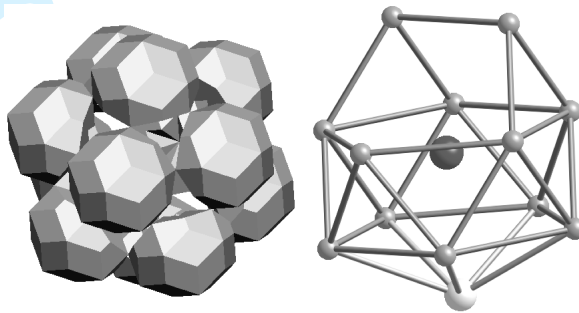


Figure 4. On the left: cell of the most frequent (69.10%) first neighbors shell chemical configuration (see table 3). On the right: the central Mn is surrounded by 7 Al on a same dodecahedron with a radius of 0.2566 nm forming a pentagon and two additional atoms and a second pentagon of Al at 0.2964 nm and finally a Pd atoms along a five fold direction. All together these atoms form a 13 atoms cage similar to an heavily deformed icosahedron with an additional vertex.

4 and table 3). This agrees with the hypothesis used by G. Trambly *et al.* [43] in their study of the electronic structure of complex Hume-Rothery phases where the Mn atoms are assumed to be embedded in an Al jellium. Hence, the effective Mn-Mn pair interaction can be computed between two non magnetic manganese atoms in an Al matrix. This effective pair interaction is strongly oscillating and present a deep minimum at 0.48 nm a next one at 0.675 nm (see figure 31 in [43]). These two distances correspond exactly to the first and second distances of the network generated by the cell α .

These results of stoichiometry and space distribution of the Mn atoms, are in good support of the α network being a reasonable idealization of the Mn chemical order in i -AlPdMn : experimental results on physical properties are very crucial data — beyond diffraction spectra — in the process of validating a structural model in quasicrystals, irrespective of final diffraction refinements.

4.2 Atomic structures of termination surfaces

Atomic models are also used to decipher the atomic structure of equilibrium termination planes of icosahedral phases if one assumes that there is little structural reconstruction and/or chemical segregation in the equilibrium surface formation with respect to the bulk structure. The main features of the numerous high quality high resolution STM images are flat terraces with well defined structures separated by steps with well defined heights (see for instance the review articles in [48]).

Generating termination planes out of a bulk model is a question of geometry as first explained by A. Katz and M. Duneau [49] in 1986. The process is two-fold: the z direction is chosen and the 6D structure is projected into the 2D-plane (z_{\parallel}, z_{\perp}). This gives the cut method scheme needed to describe the step heights between terraces. Then, all AS's are cut by this 2D-plane leading to a set of polygons in a 4D-space and

10

1
2
3
4
5
6
7
8
9
10
11
12
13
14
15
16
17
18
19
20
21
22
23
24
25
26
27
28
29
30
31
32
33
34
35
36
37
38
39
40
41
42
43
44
45
46
47
48
49
50
51
52
53
54
55
56
57
58
59
60

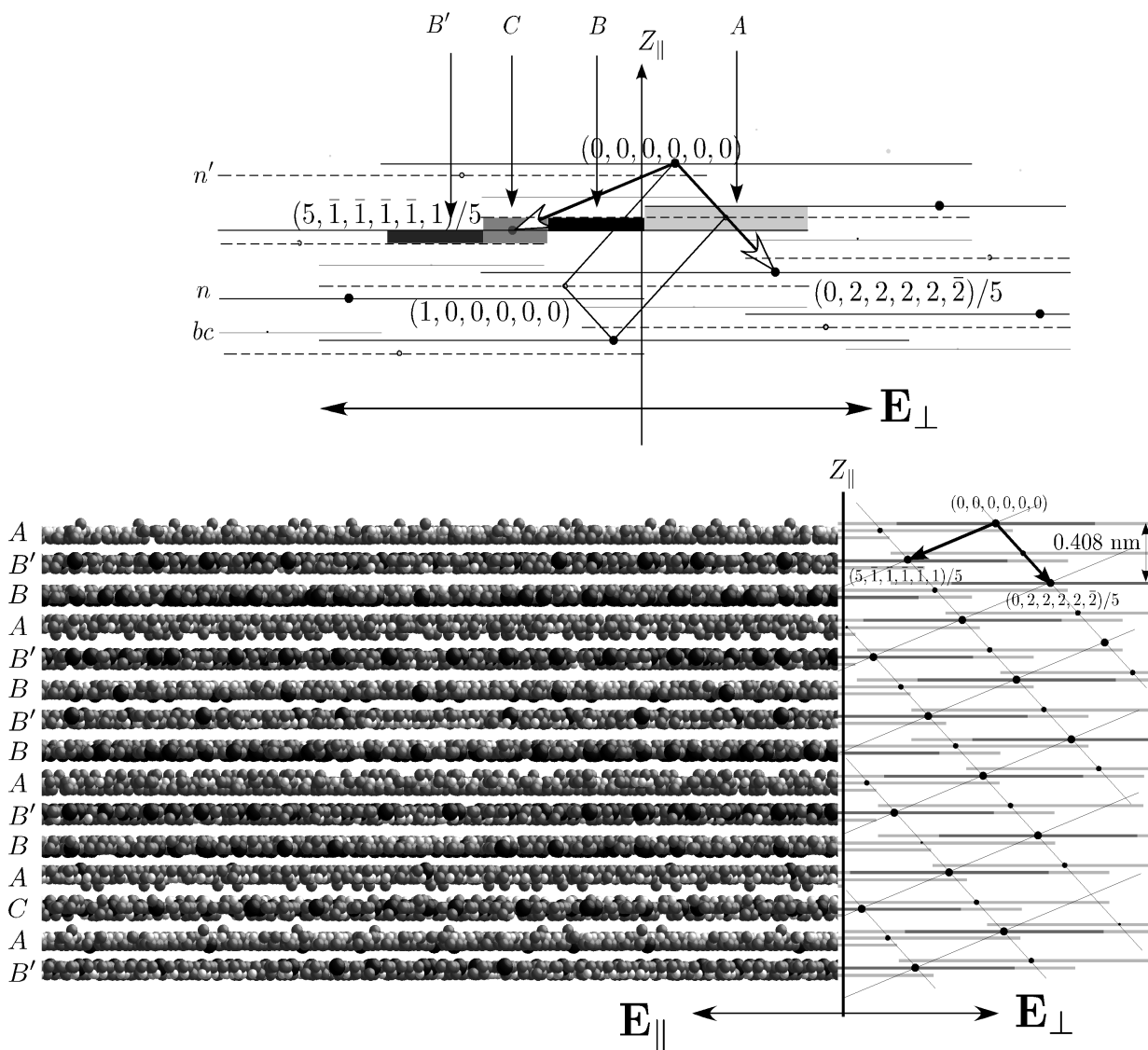


Figure 5. On top: projection of the AS's into a 5-fold 2D plane. The projected structure is made of three AS's that are the traces of the convex envelopes of the n , n' and bc ASs. The trace of n is represented by thick lines, the trace of n' is drawn as dashed thick lines and of bc as thin lines. Plausible termination surfaces can form in collapsing two or three planes close to each others (0.048 nm) issued from n and n' : there are essentially four different possible cases $A B B'$ and C . On bottom: correspondence between the 2D cut and the atomic structure seen perpendicular to the 5-fold direction shows how the atomic planes can be grouped into doublets and triplets. For clarity, the bc AS has not been included in the generation of the model. Large black spheres correspond to Mn, small grey ones to Al, and small white ones to Pd.

a 4D-lattice out of which the actual 2D-surface structure is generated by the usual cut method from 4 to 2 dimensions.

We designate by $\{|i\rangle\}$ the canonic 6D natural basis and by $\{|\alpha\rangle\}$ and $\{|\bar{\alpha}\rangle\}$ two 3D orthonormal bases spanning respectively E_{\parallel} and E_{\perp} . The entire geometry is defined by the scalar products $\langle\alpha|i\rangle$ and $\langle\bar{\alpha}|i\rangle$ that give the coordinates of the unit vectors $\{|\alpha\rangle\}$ and $\{|\bar{\alpha}\rangle\}$ on the canonical basis. The projectors on the subspaces E_{\parallel} and E_{\perp} are thus defined by $\hat{\pi}_{\parallel} = \sum_{\alpha=x,y,z} |\alpha\rangle\langle\alpha|$ and $\hat{\pi}_{\perp} = \sum_{\bar{\alpha}=x',y',z'} |\bar{\alpha}\rangle\langle\bar{\alpha}|$ with the closure condition $\hat{\pi}_{\parallel} + \hat{\pi}_{\perp} = \hat{1}$.

Let $|U\rangle$ be a rational direction of the 6D lattice. The rational 2D-plane associated to $|U\rangle$ is generated by the projections of $|U\rangle$ in E_{\parallel} , $|U_{\parallel}\rangle = \hat{\pi}_{\parallel}|U\rangle$ and in E_{\perp} , $|U_{\perp}\rangle = \hat{\pi}_{\perp}|U\rangle$. This 2D plane is therefore defined by the projector $\hat{\pi}^U = |U_{\parallel}\rangle\langle U_{\parallel}| + |U_{\perp}\rangle\langle U_{\perp}|$ after $|U_{\parallel}\rangle$ and $|U_{\perp}\rangle$ are normalized, $\langle U_{\parallel}|U_{\parallel}\rangle = \langle U_{\perp}|U_{\perp}\rangle = 1$.

Another equivalent way¹ of defining the 2D-plane, consists in adding to $|U\rangle$, its transformed by qua-

¹This technic is better for characterizing the position of the projected 6D nodes in the 2D-plane with respect to two simple vectors of

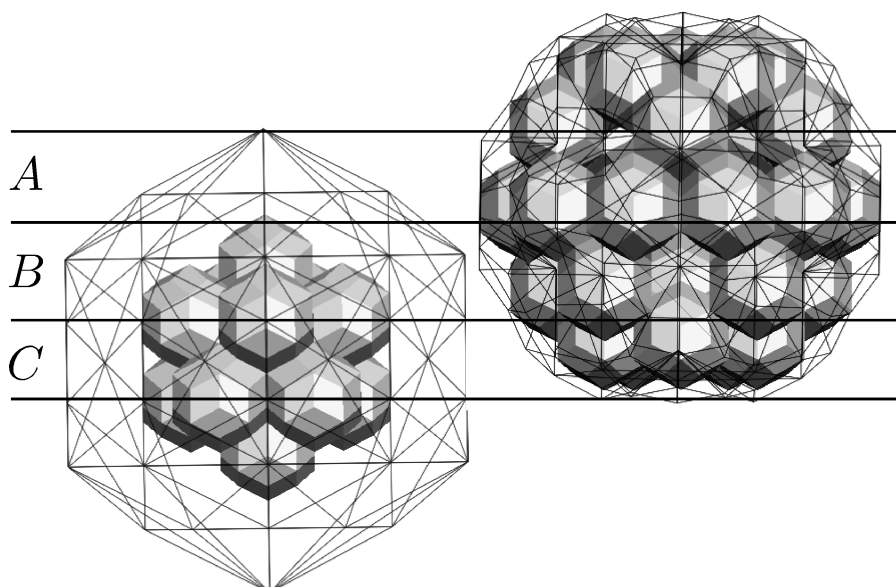


Figure 6. The two main ASs n on the left and n' on the right properly displaced with respect to each other (see figure 5) with their inner polyhedra oriented with a 5-fold axis along the vertical direction. A , B and C type termination planes are obtained by cuts made in respectively the A , B and C regions.

sidilatation defined by $|V\rangle = \hat{\mathbf{T}}|U\rangle = \tau\hat{\pi}_{\parallel}|U\rangle + (1 - \tau)\hat{\pi}_{\perp}|U\rangle$ and constructing the projector using two orthogonal vectors of the plane, for example $|U\rangle$ and $|W\rangle = |U\rangle/\langle U|U\rangle - |V\rangle/\langle U|V\rangle$. This leads to the projector $\hat{\pi}^U = |U\rangle\langle U| + |W\rangle\langle W|$ again after $|U\rangle$ and $|W\rangle$ are normalized².

In the case of the 5-fold orientation, the 2D-plane is spanned by the two vectors $|1, 0, 0, 0, 0\rangle$ and $1/\sqrt{5}|0, 1, 1, 1, 1, \bar{1}\rangle$ defining the projector $\hat{\pi}_5 = |1, 0, 0, 0, 0\rangle\langle 1, 0, 0, 0, 0| + \frac{1}{5}|0, 1, 1, 1, 1, \bar{1}\rangle\langle 0, 1, 1, 1, 1, \bar{1}|$. The resulting projected structure is shown on figure 5; it has a 2D lattice with unit vectors $u = 1/5(5, \bar{1}, \bar{1}, \bar{1}, \bar{1}, 1)$ and $v = 1/5(0, 2, 2, 2, 2, \bar{2})$ that is the τ -inflated vector of u . The traces of the ASs are represented as horizontal lines (thick full line for n , dashed one for n' and thin line for bc). Once a z -direction is chosen, the intersection of that direction with the ASs (horizontal lines on figure 5) cuts the AS polyhedra as polygons, the area of which are proportional to the atomic density of the planes.

A first remarkable fact is that any given single flat 5-fold plane is generated by one and only one kind of AS, either n , n' or bc so that each 5-fold plane can be characterized by one kind of AS: n , n' and bc planes (the bc planes have very low density and will not be discussed here). It can be shown on the projection (see figure 5) that n and n' ASs generate packs of parallel planes stacked at very close distances (0.048 nm in the bulk) from each others and that they can be grouped together to form one unique slightly corrugated (irrespective of surface relaxation) termination plane. Figure 5 shows that there are essentially four different plausible solutions for forming those dense thick termination planes: A that results in the close superimposition of three planes ($n|n'|n$), B resulting in the superimposition of two planes ($n'|n$), and B' corresponding to the opposite ($n|n'$), and finally C corresponding to ($n'|n|n'$).

As in the previous section, these all features are roughly independent of the models. As soon as these models have the two main ASs at n and n' , the overall geometry is given by the drawings of figure 5, with little variations. So, doublets and triplets of close planes are solid structural features well recognized by the surface science community [50–53]. But, here again the question of the chemical composition is opened (see the article of P. Thiel in this issue).

In our model, as shown on figure 6, the solution A , corresponds to a termination plane containing atoms generated by the periphery of the n AS and the center of the n' AS. The cuts are located in the A region of figure 6 at z -levels higher than the topmost vertex of the α cell that generates Mn atoms. Therefore, the n AS generates essentially Al atoms. The cut of the n' AS occurs close to the equatorial plane where

that plane.

²In both cases, the complementary 4D space, say P_U , is defined by the projector $\hat{\pi}^{P_U} = \hat{\mathbf{1}} - \hat{\pi}^U$.

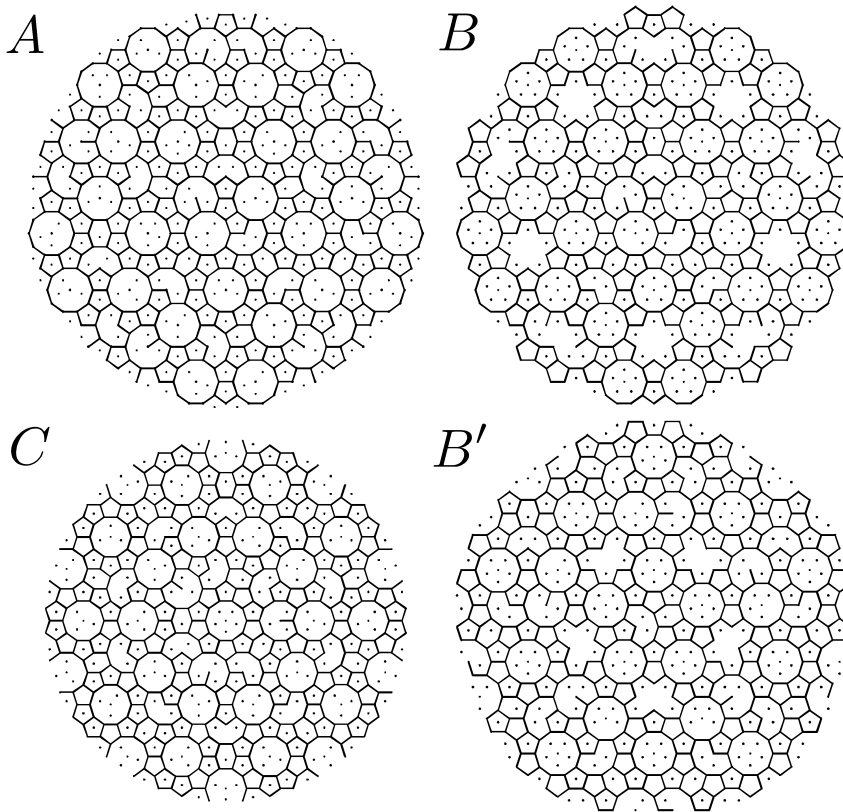


Figure 7. The four main possible termination planes obtained by collecting two or three planes that are 0.048 nm apart from each other in the bulk structure: *A* is the result of collapsing three close planes ($n|n'|n$), *B*, two planes ($n'|n$) and *B'* the opposite ($n|n'$) and *C* three planes ($n'|n|n'$). To highlight the geometrical skeleton of the planes, Al atoms that are 0.29 nm away from each other are linked by thin bars.

the β cell has a maximum area: the contribution of n' is therefore a mixture of Al and Pd in roughly equal proportions. Using the same kind of qualitative argumentation, we see that the solutions *B* and *B'* involve inner shells of both n and n' ASs. This leads to termination planes made of a mixture of all three chemical species. Finally, solution *C* corresponds to the center of n and the periphery of n' leading to a mixture of all three chemical species but with a large proportion of Mn and Pd.

Typical examples of these four termination planes are given on figure 7. The sequences of the terrace steps are predicted by a cut method applied to the 2D-plane shown on the bottom of figure 5. All steps height are here of the form $\tau^n h_0$ where h_0 is the length of the projection in \mathbf{E}_{\parallel} of the vector u (here $h_0 = 0.252$ nm for i -AlPdMn). Because v is the τ -inflated of u the step heights should be of the form $(n + m\tau)h_0$ with n and m integers. The densest termination surface is obtained for case *A*, *i. e.* a contraction of three planes ($n|n'|n$). Under that simplified hypothesis, the steps heights take essentially the two values 0.408 and 0.66 nm in a stacking close to Fibonacci sequence and the composition of the termination planes is an Al rich mixture of Al and Pd.

5 Conclusion

The question of the atomic structure determination of quasicrystal has considerably progressed during these 25 years but uncertainties are still present concerning the chemical order. The first observation by M. Cornier-Quiquandon *et al.* [41] of the diffraction intensities of i -AlCuFe that split into four well defined branches according to the parity of the characteristic numbers [35] N and M of the reflections, has led to the determination of the locations of the main atomic surfaces at n , n' and secondary ones at bc and possibly me . This primary fact is strongly experimentally established and verified for all presently known icosahedral phases. It is the main reason for all actual models to have roughly 85% of the atom locations in common.

On the other hand, the determination of the chemical order is a much more difficult task and significant discrepancies still exist on this point between the various models. Refinements of the diffraction data lead to very accurate structural solutions that can unfortunately not be proven as unique. Other solutions like High Resolution Electron Microscopy techniques are very powerful for revealing the quasiperiodic geometry of the atomic network but are of insufficient sensitivity to differentiate several models that give similar projections (see M. Quiquandon & D. Gratias in this issue). Finally, the STM technique can ultimately characterize the composition of the termination plane that is unfortunately not necessary the composition of the bulk.

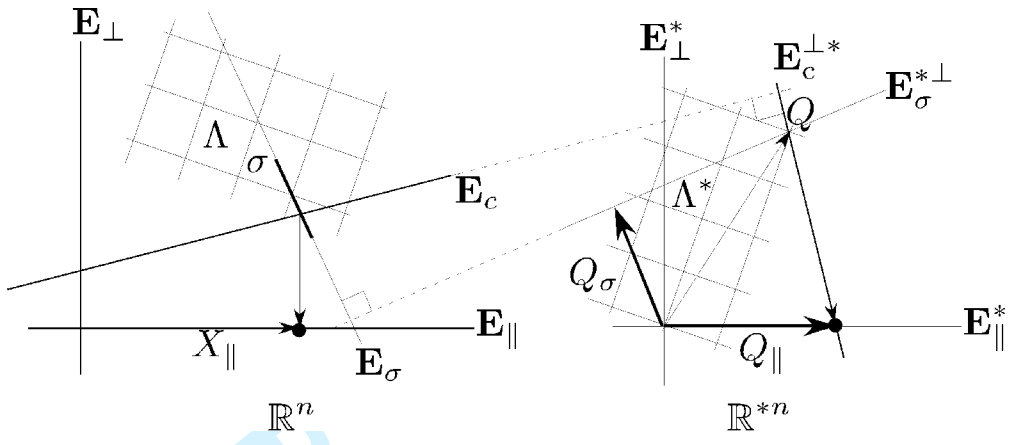
It is therefore clear that additional works have to be pursued inside and outside the classical tools of crystallography. For example, cohesive energy calculations of approximant phases as function of chemical ordering, spectroscopies and physical properties measurements sensible to local configurations should play a key role for eventually leading to unambiguous and fully accepted crystallographic descriptions of these astonishing phases.

References

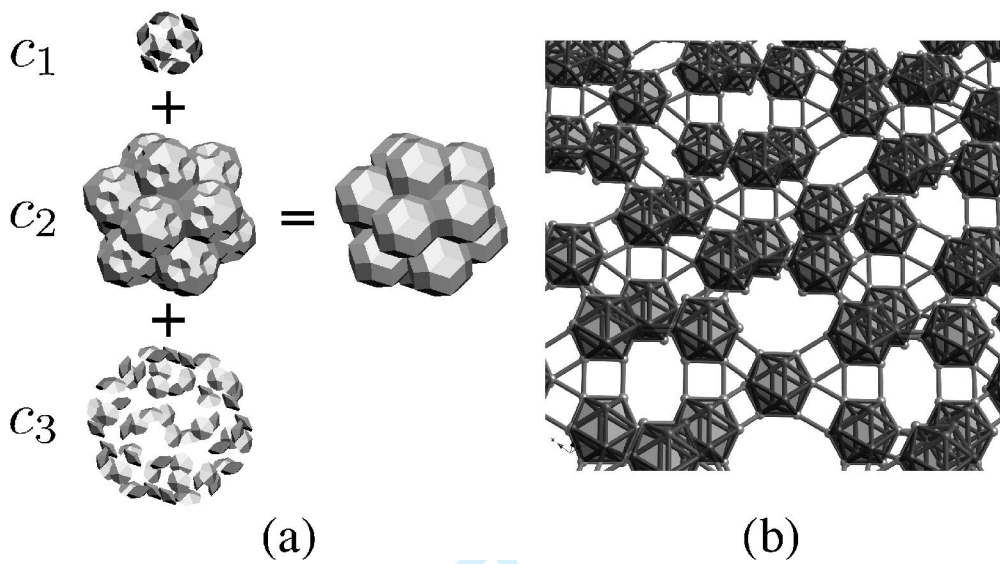
- [1] D. Shechtman, I. Blech, D. Gratias and J.-W. Cahn, *Phys. Rev. Lett.*, **53**, 1951—1955 (1984)
- [2] D. Levine & P. Steinhardt, *Phys. Rev. Lett.*, **53**, 2477—2480 (1984).
- [3] H. Bohr *Acta Math.*, **45**, 29—127 (1924); **46**, 101—214 (1925); **47**, 237—281 (1926).
- [4] A.S. Besicovic, *Almost Periodic Functions*, Cambridge University Press, Cambridge (1932).
- [5] M. Senechal, *Notices of the AMS*, **53**, n 8, 886—887 (2006)
- [6] International Union of Crystallography, *Acta Crystallographica A* **48**922 (1992).
- [7] D. Mermin, *Methods of structural analysis of modulated structures and quasicrystals*, J.-M. Perez-Mato, F. J. Zuniga and G. Madariaga eds, World Scientific Singapore, 129—184 (1991).
- [8] G. Bernuau & M. Duneau, *Directions in mathematical quasicrystals*, M. Baake and R. V. Moody, CRM monographs series **13**, 43—60 (2000).
- [9] A. Yamamoto, H. Takakura & A.-P. Tsai, *Phys. Rev. B* **68**, 094201 (2003).
- [10] M. Quiquandon & D. Gratias, *Phys. Rev. B* **74**, 214205 (2006).
- [11] D. Shechtman and I. A. Blech, *Metallurgical Transaction A*, **16A**, 1005—1012 (1985)
- [12] M. Duneau & A. Katz, *Phys. Rev. Lett.* **54**, 2688—2691 (1985).
- [13] V. Elser, *Phys. Rev. B* **32**, 4892 — 4898 (1985); *ibid*, *Acta Crystallogr A* **42**, 36 (1986).
- [14] P. A. Kalugin, A. Yu Kitaev & L. C. Levitov, *Pis'ma Zh. Eksp. Teor. Fiz.* **41** 119 (1985) [*JETP Lett.* **41**, 119 (1985)].
- [15] P. Bak, *Phys. Rev. Lett.* **54**, 1517—1519 (1985).
- [16] P. Bak, *Phys. Rev. B* **32**, 5764—5772 (1985).
- [17] A. Janner & T. Janssen, *Phys. Rev. B* **15**, 643 (1977).
- [18] P. M. de Wolff, *Acta Cryst. A* **33** 609 (1977).
- [19] D. Gratias, J.-W. Cahn & B. Mozer, *Phys. Rev. B* **38**, 1643 (1988).
- [20] L. Pauling, *Nature*, **317**, 512—514 (1986); L. Pauling, *Phys. Rev. Lett.*, **58** 4, 365—368 (1987); see answers by J.-W. Cahn, D. Gratias, D. Shechtman, A. L. Mackay, P.A. Bancel, P. W. Stephens, A. Goldman & A.A. Berezin, in *Nature*, **319**, No 6049, 102—104 (1986).
- [21] P. W. Stephens & A. I. Goldman *Phys. Rev. Lett.* **56** No11 1168—1171 (1986).
- [22] S.-Y. Qiu & M.V. Jaric, *Quasicrystals*, M.V. Jaric, S. Lundqvist Edts, World Scientific, Singapore, (1990).
- [23] L.-H. Tang & M. V. Jaric, *Proceedings of the Anniversary Adriatic Research Conference on Quasicrystals* edited by M.V. Jaric and S. Lundqvist (World Scientific, Singapore, 1990), pp 319—336.
- [24] M. Widom, *Proceedings of the Anniversary Adriatic Research Conference on Quasicrystals* edited by M.V. Jaric and S. Lundqvist (World Scientific, Singapore, 1990), pp 337—355.
- [25] C. L. Henley, *Quasicrystals: The State of the Art* edited by P. J. Steinhardt and D. P. Divincenzo (World Scientific, Singapore, 1991), pp 429—518.
- [26] C. L. Henley, V. Elser, & M. Mihalkovic, *Z. Kristallogr* **216** 1—14 (2001).
- [27] P. Gummelt *Proceedings of the 5th International Conference on Quasicrystals* edited by C Janot and R. Mosseri (World Scientific, Singapore, 1995), pp 84—87.
- [28] P. Gummelt *Geometriae Dedicata* **62**, (1996).
- [29] F. Ghler *Quasicrystals, Current Topics* edited by E. Belin-Ferr, C. Berger, M. Quiquandon and A. Sadoc (World Scientific, Singapore, 2000), pp 118—127.
- [30] F. Ghler, P. Gummelt & S. I. Ben-Abraham *Coverings of Discrete Quasiperiodic Sets, Theory and Applications to quasicrystals* edited by P. Kramer and Z. Papadopolos (Springer, Berlin, 2003), pp 63—93.
- [31] P. Kramer *Coverings of Discrete Quasiperiodic Sets* edited by P. Kramer and Z. Papadopolos (Springer, Berlin, 2003), pp 1—18; pp 97—163.
- [32] W. Steurer, *Z. Kristallogr.* (2004) 391-446.
- [33] P. Bak, *Phys. Rev. Lett.* **56**, 861—864 (1986).
- [34] V. Elser, *Phys. Rev. B* **82**, 4892 (1985).
- [35] J. W. Cahn, D. Shechtman & D. Gratias, *J. Mater. Res.* **1**, 13—26 (1986).
- [36] A. Bienenstock & P.P. Ewald, *Acta Cryst.* **15**, 1253 (1962).
- [37] D. Frenkel, C. L. Henley and E.D. Siggia, *Phys. Rev. B* **34**, 3649—3669 (1986).
- [38] A. Katz & D. Gratias in *Lectures on Quasicrystals*, edited by F. Hippert and D. Gratias (Les Editions de Physique, Les Ulis, 1994), pp 187—264 (1994).
- [39] A. Katz in *Beyond Quasicrystals*, edited by F. Axel and D. Gratias (Les Editions de Physique-Les Ulis Springer Verlag Berlin Heidelberg New York), 141—189 (1995).
- [40] D. Gratias, A. Katz & M. Quiquandon, *J.Phys.: Condens. Matter* **7**, 9101—9125 (1995).

- 1 [41] M. Cornier-Quiquandon, A. Quivy, S. Lefebvre, E. Elkaim, G. Heger, A. Katz and D. Gratias, *Phys. Rev. B* **44** n 5 2071-2084 (1991).
2 [42] M. Boudard, M. de Boissieu, C. Janot, G. Heger, C. Beeli, H.-U. Nissen, H. Vincent, R. Ibberson, M. Audier & J.-M. Dubois J.
3 *Phys. Condens. Matter* **4**, 10149 (1992).
4 [43] G. Trambly de Laissardire, D. Nguyen-Manh and D. Mayou, *Progress in Materials Science* **50**, (2005), 679–788.
5 [44] J. J. Préjean, C. Berger, A. Sulpice and Y. Calvayrac, *Phys. Rev. B*, **65**, 140203-1–4, (2002).
6 [45] F. Hippert, M. Audier, J. J. Préjean, A. Sulpice, E. Lhotel, V. Simonet and Y. Calvayrac, *Phys. Rev. B*, **68**, 134402-1–13, (2003).
7 [46] F. Hippert, M. Audier, J.-J Préjean, A. Sulpice,, V. Simonet and Y. Calvayrac, *J. of Non-Crystalline Solids*, **334 & 335**, 403–407,
8 (2004).
9 [47] J.-J Préjean, E. Lhotel, A. Sulpice & F. Hippert, *Phys. Rev. B*, **73**, 214205 (2006).
10 [48] *Progress in Surface Science*, special issue Quasicrystals, **75** 3–8 (2004).
11 [49] A. Katz and M. Duneau, *J. Physique* **47** 181-186 (1986).
12 [50] M. Gierer, M. A. Van Hove, A. I. Goldman, Z. Shen, S.-L. Chang, P. J. Pinheor, C. J. Jenks, J. W. Anderegg, C.-M. Zhnag & P. A.
13 Thiel, *Phys. Rev. B* **57** 13, 7628—7641 (1998).
14 [51] L. Barbier, D. Le Floch, Y. Calvayrac & D. Gratias, *Phys. Rev. Lett* **88**, 85506 (2002).
15 [52] Z. Papadopolos, G. Kasner, J. Ledieu, E. J. Cox, N. V. Richardson, Q. Chen, R. D. Diehl, T. A. Lograsso, A. R. Ross & R. McGrath,
16 *Phys. Rev. B*, **66**, 184207 (2002).
17 [53] Z. Papadopolos, P. Pleasants, G. Kasner, V. Fournée, C. J. Janks, J. Ledieu & R. MacGrath, *Phys. Rev. B* **69**, 224201 (2004).
18
19
20
21
22
23
24
25
26
27
28
29
30
31
32
33
34
35
36
37
38
39
40
41
42
43
44
45
46
47
48
49
50
51
52
53
54
55
56
57
58
59
60

1
2
3
4
5
6
7
8
9
10
11
12
13
14
15
16
17
18
19
20
21
22
23
24
25
26
27
28
29
30
31
32
33
34
35
36
37
38
39
40
41
42
43
44
45
46
47
48
49
50
51
52
53
54
55
56
57
58
59
60

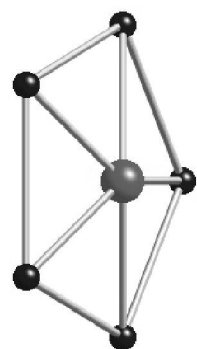
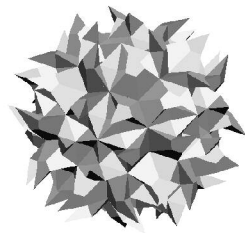
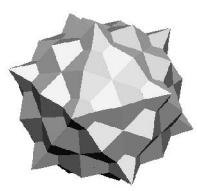
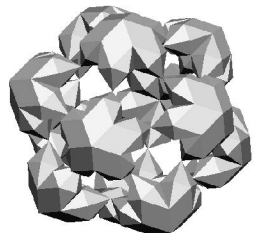


Peer Review Only

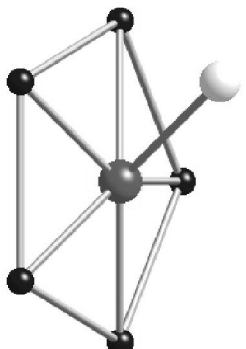


Review Only

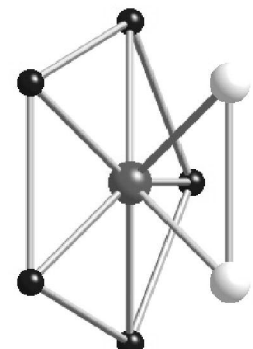
1
2
3
4
5
6
7
8
9
10
11
12
13
14
15
16
17
18
19
20
21
22
23
24
25
26
27
28
29
30
31
32
33
34
35
36
37
38
39
40
41
42
43
44
45
46
47
48
49
50
51
52
53
54
55
56
57
58
59
60



C₁

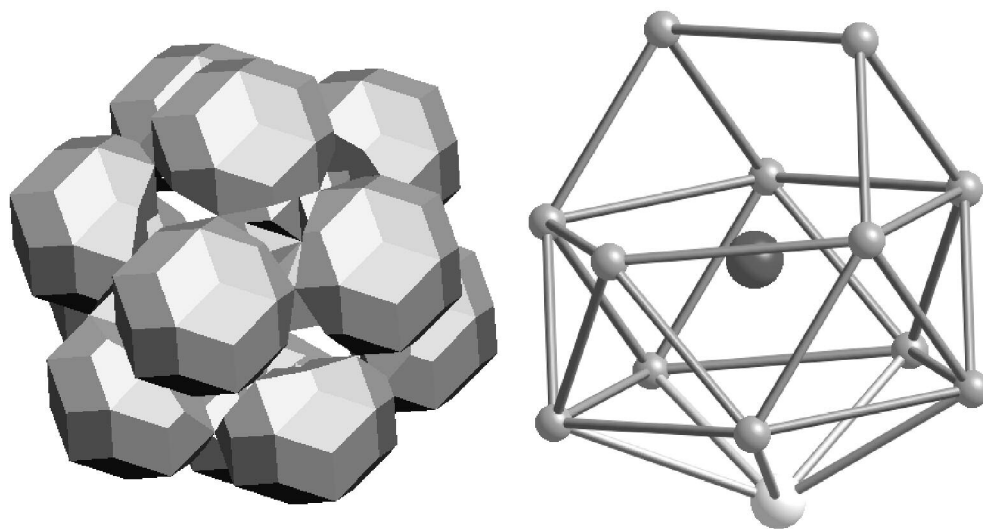


C₂



C₃

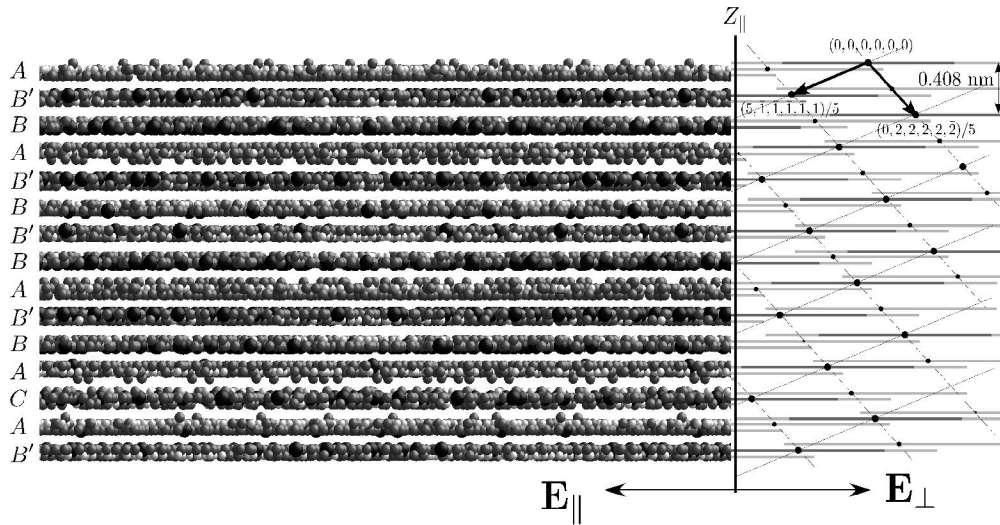
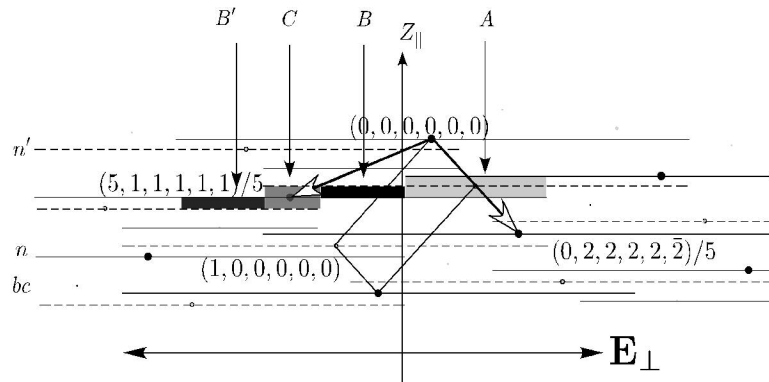
Review Only



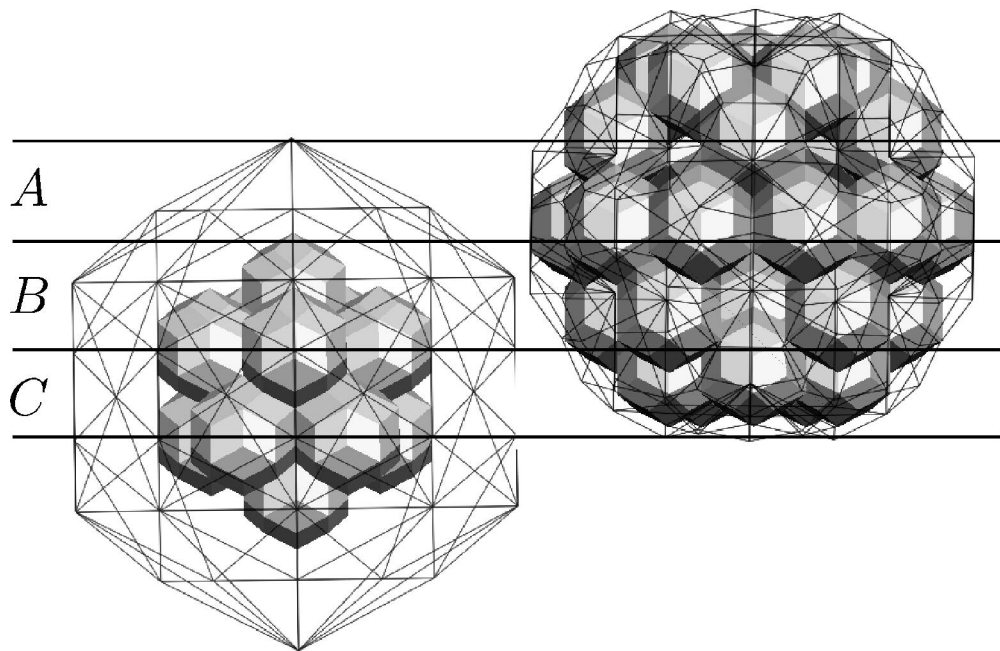
er Review Only

1
2
3
4
5
6
7
8
9
10
11
12
13
14
15
16
17
18
19
20
21
22
23
24
25
26
27
28
29
30
31
32
33
34
35
36
37
38
39
40
41
42
43
44
45
46
47
48
49
50
51
52
53
54
55
56
57
58
59
60

1
2
3
4
5
6
7
8
9
10
11
12
13
14
15
16
17
18
19
20
21
22
23
24
25
26
27
28
29
30
31
32
33
34
35
36
37
38
39
40
41
42
43
44
45
46
47
48
49
50
51
52
53
54
55
56
57
58
59
60



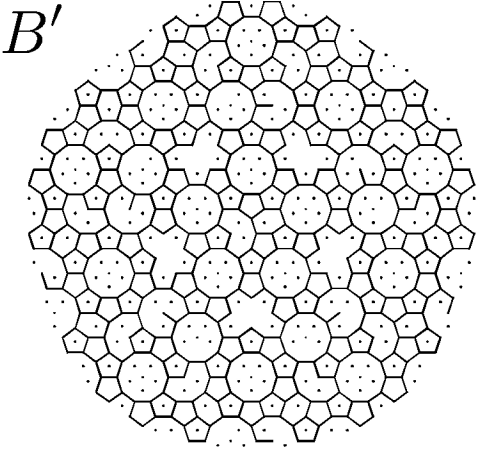
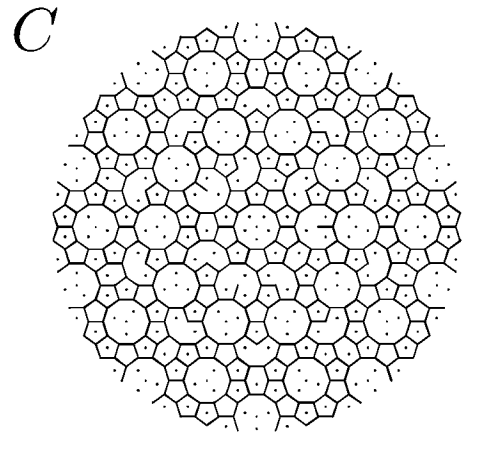
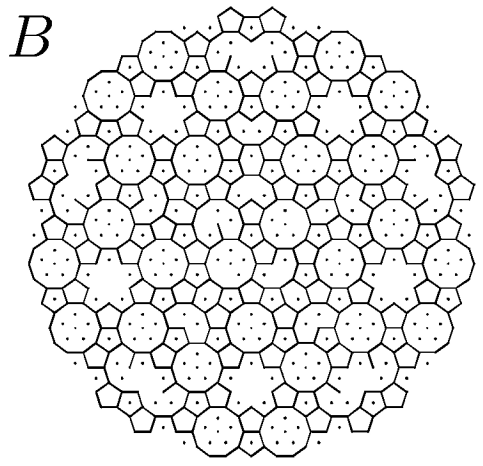
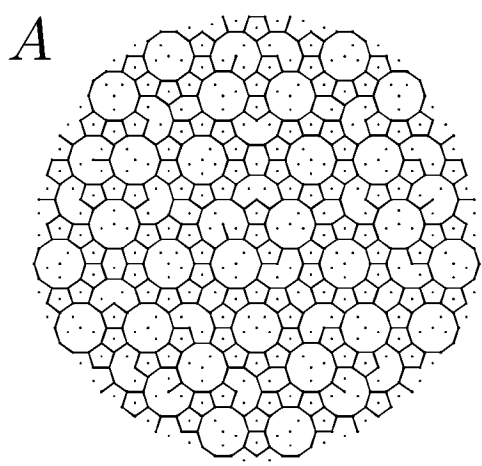
www Only



Review Only

1
2
3
4
5
6
7
8
9
10
11
12
13
14
15
16
17
18
19
20
21
22
23
24
25
26
27
28
29
30
31
32
33
34
35
36
37
38
39
40
41
42
43
44
45
46
47
48
49
50
51
52
53
54
55
56
57
58
59
60

1
2
3
4
5
6
7
8
9
10
11
12
13
14
15
16
17
18
19
20
21
22
23
24
25
26
27
28
29
30
31
32
33
34
35
36
37
38
39
40
41
42
43
44
45
46
47
48
49
50
51
52
53
54
55
56
57
58
59
60



Manuscript Only

P.1

- 8 Structure of quasicrystals: where are the atoms *{omit space before :}*
- 19 Abstract 5 *{I suggest}* ...quasicrystals: we do have quite a solid idea of where the atoms are but we are not sure about the distribution of the chemical species.
- 30 A. Besicovic → A.S. Besicovitch *{also in Ref [4]}*
- 32 define → defines
- 37 N -dim → N -dimensional *{spell out}*
- 45 tractable- → tractable - *{insert space}*
- 49 works → studies
- 52-53 differ on ... → differ in some details they all agree on the location ...
- 54 opened → open
- 58 Various... → Various models although showing similar diffraction patterns
Differ on the chemical decoration of the atomic sites

P.2

- 3 with → by
- 4 *{suggest}* (Al-Mn) alloy → **Al-Mn** alloy *{that's the usual standard, but you might just omit the parentheses}*
- 12 cut and project → cut-and-project
- 20 N -dim → N -dimensional *{spell out}*
- 21 should stabilized → should be stabilized
- 30 combination → combinations
- 30 basic... → base vectors e_i *{or \vec{e}_i }*
- 31 *{analogous but}* \sum_i^N → \sum_i^6 *or simply \sum_i*
- 33 diffraction → a diffraction
- 33 well-defined → well defined

P.3

- 8 Non crystallographic → Non-crystallographic
- 10 Non crystallographic → Non-crystallographic
- 28 N -dim → N -dimensional *{spell out}*
- 37 euclidean → Euclidean *{or consistently decapitalize}*
- 39ff *{q, t are vectors: $\vec{q}_\perp \cdot \vec{t}_\perp$ 'the dot is raised'}*
- 39 N -dim → N -dimensional *{spell out}*
- 44 an unit → a unit
- 48 $(N - D)$ -dim → $(N - D)$ -dimensional *{spell out}*
- 51 issued → inferred

P.4

- 3 *{suggest}* A large amount of work has been dedicated to the geometrical constraints on ASs.
- 11 $N - D$ → $(N - D)$ -dimensional

P.5

- 13-14 on → On
 36 starting early ...for → starting in the early '90s with
 38ff *{again the Qs and Rs are vectors}*
 51 AS → ASs
 57 an usual → a usual
 58 This fact → The fact

P.6

- 28 are → take
 34 $A \rightarrow a$
 44 $-1 \rightarrow -1$

P.7

- 32 opened → open
 48 distribute → are distributed
 57-68 a too small value for being experimentally measured. → a value too small to be measured experimentally.
 59 bounds → bonds

P.8

- 6 neighbors → neighbor

P.10

- 38 On top → Top *{suggest}*
 40 On bottom → Bottom *{suggest}*
 41 grey → gray *{author uses US spelling}*

P.11

- 34 As's → ASs
 46 these all → all these
 49 opened → open

P.13

- 5 technics → techniques
 5 powerfull → powerful
 7 technic → technique
 8-9 not necessary → not necessarily
 10 ...additional works have to be pursued inside and outside → additional work has to be done both within and without
 11ff *{suggest}* For example, calculation of the cohesive energy of approximant phases as a function of chemical ordering, as well as spectroscopy and measurement of physical properties sensible ...
 21 AS. Besicovic → A.S. Besicovitch
 and in all page citations: – → -